On the Effect of RIS Phase Quantization on Communications System Performances

Abdullah Haskou, Hamidreza Khaleghi

On the Effect of RIS Phase Quantization on Communications System Performances

Abdullah Haskou, Hamidreza Khaleghi
b<>com
1219 Avenue des Champs Blancs, 35510 Cesson-Sévigné, France
Email: {abdullah.haskou, hamidreza.khaleghi}@b-com.com

***Abstract*—The past wireless communication systems were designed taking the channel as an uncontrollable element and optimizing the system around this element. However, recently Reconfigurable Intelligent Surfaces (RISs) have gained a significant interest as a way to control the wireless propagation environment and improve the communication system performances. However, to achieve optimal performances, a continuous-phase RIS is required. But, the practical realization of RISs makes it very difficult to obtain a RIS with more than few phase states. Therefore, the required RIS phase must be quantized to these available states. In this paper, we investigate the effect of RIS phase quantization on the wireless system performances in terms of RIS beamforming capabilities, received signal level, and channel estimation accuracy compared to a continuous-phase RIS. We demonstrate that starting from 2-bit quantization very good performances can be achieved.**

Keywords—Reconfigurable Intelligent Surface (RIS), phase-quantization, quantization loss

I. INTRODUCTION

A Reconfigurable Intelligent Surface (RIS) is a programmable structure that can be used to control electromagnetic (EM) waves' propagation [1]. Indeed, a RIS is a planar surface made of an array of passive reflecting elements, each of which can independently impose the required phase shift on the incoming signal. By carefully adjusting the phase shifts of all the reflecting elements, the reflected signals can be configured to propagate in the desired direction [2-5]. Furthermore, RISs can operate in full-duplex (FD) mode, meaning that they can provide two-way communications [6] via symmetrical beams. RISs' types include reflecting surfaces, refracting surfaces, focusing surfaces, absorbing surfaces and others. RISs can be passive (without amplification) or active (with amplification). Previous generations of wireless systems were designed by considering the wireless propagation channel as an uncontrollable factor and optimizing the system around this factor. However, recently, RISs have gained a significant interest as a way to control the wireless propagation channel and improve the wireless system performances. Indeed, RISs can be used for coverage enhancement, localization and sensing, energy saving, etc. In [7], an overview of RIS enabled opportunities for 5G-Advanced is provided and some critical requirements and challenges are highlighted from a standardization perspective. The latest progress in research, development and standardization on RISs is presented in [8]. Several works have studied practical implementations of discrete-phase RIS. In [9], the authors reported early field trial results of RISs in 5G networks. The experimental results showed that RISs can solve coverage issues and improve received signal quality in 5G networks across different frequency bands. However, to achieve the best wireless system performances, a continuous-phase RIS is required. Meanwhile, the practical realization of RIS tend towards n-bit quantized RIS (that has 2^n phase states). In [10], the authors proposed a method to minimize the transmit power in wireless communications assisted by discrete RIS by jointly optimizing the continuous transmit beamforming at the transmitter and discrete reflect beamforming at the RIS, subject to a given Signal-to-Noise Ratio (SNR) constraint at the receiver. In [11], the authors investigated RIS discrete phase shifting method to reduce the network overhead of RIS-aided multiple-antenna systems.

In this paper, we evaluate the effect of RIS phase quantization on the wireless system performances in terms of RIS beamforming capabilities, received signal level, and channel estimation accuracy compared to a continuous-phase RIS. We demonstrate that starting from 2-bit quantization very good performance can be obtained with less than 1 dB degradation in the received power level due to quantization loss.

The rest of the paper is organized as follows. Section II introduces a brief theoretical background. Section III analyzes the effect of RIS phase quantization on the system performances. Section IV introduces the simulation results. Finally, Section V presents some conclusions.

Notations: We use the following notations throughout this paper. We represent Matrices by bold uppercase letters and vectors by bold lowercase letters. Superscripts T, H and -1 denote the transposition, Hermitian transposition, and inversion operations. $diag(\boldsymbol{x})$ returns a square diagonal matrix with the elements of vector $\boldsymbol{x}$ on the main diagonal.

II. THEORATICAL BACKGROUND

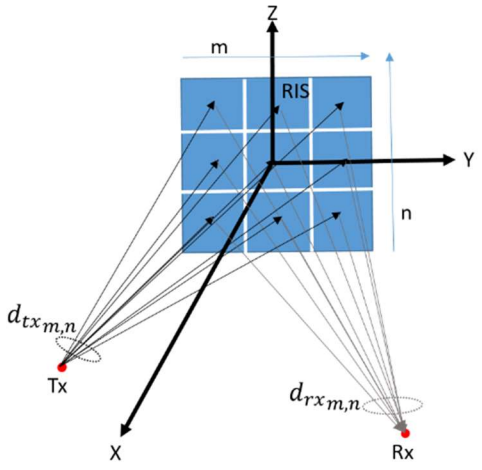

Figure 1. An example of a RIS-aided communication system.

Let us consider a RIS-aided communication system consisted of a transmitter (Tx), a reciever (Rx), and a RIS composed of multiple elements *(m,n)* as shown in Figure 1 (the figure is not to scale, but rather a schematic representation). Let us also denote the complex reflcetion coefficient of every RIS elements by:

$$\Gamma_{m,n} = \left|\Gamma_{m,n}\right| e^{j\varphi_{m,n}} \quad (1)$$

where $\left|\Gamma_{m,n}\right|$ is the reflection magnitude and $\varphi_{m,n}$ is the reflection phase.
Assuming the reflection magnitude of all the RIS elements is unity (i.e., $\left|\Gamma_{m,n}\right| = 1$), the complex reflection coefficient can be reduced to:

$$\Gamma_{m,n} = e^{j\varphi_{m,n}} \quad (2)$$

Considering that the RIS is in the far-field region of both the transmitter and the reciever, and that there is only a Line of Sight (LoS) path from- and to- the RIS (for an antenna with biggest dimension *D*, the inner radius of far-field region is given by $R = \frac{2D^2}{\lambda}$ [12]). Using free-pace propagation model with far-field approximations and ignoring the additive noise, the recived signal is given by:

$$s_{rx} = \frac{s_{tx}\lambda^2\sqrt{G}}{(4\pi)^2 d_{tx} d_{rx}} \sum_{m=1}^{M}\sum_{n=1}^{N} e^{j\left(\varphi_{m,n} - k\left(d_{tx_{m,n}} + d_{rx_{m,n}}\right)\right)} \quad (3)$$

where s_{tx} is the trasmitted complex signal, λ is the free-space wavelength, $k = \frac{2\pi}{\lambda}$ is the wave number, d_{tx} , d_{rx} are respectively the distance from the RIS central element to Tx and Rx, and $d_{tx_{m,n}}$, $d_{rx_{m,n}}$ are the distance from the *(m,n)* element respectively to Tx and Rx, and G represents the oevrall gain between Tx and Rx through RIS.

To maximize the received signal's amplitude, all signals reflected by RIS elements must arrive in phase at the receiver. Hence:

$$\varphi_{m,n} - k\left(d_{tx_{m,n}} + d_{rx_{m,n}}\right) = \varphi_0 \quad (4)$$

$$\rightarrow \varphi_{m,n} = \varphi_0 + k\left(d_{tx_{m,n}} + d_{rx_{m,n}}\right) \quad (5)$$

By setting $\varphi_0 = 0$, the required phase for *(m,n)* element is given by [3]:

$$\varphi_{m,n} = k\left(d_{tx_{m,n}} + d_{rx_{m,n}}\right) \quad (6)$$

Substituting (6) in (3), the received signal is given by:

$$s_{rx} = \frac{s_{tx} NM\sqrt{G}\lambda^2}{(4\pi)^2 d_{tx} d_{rx}} \quad (7)$$

This equation shows that the received signal's amplitude increases propotionally to the number of RIS elements ($N \times M$). Or equivalently, the received signal's power and SNR increase quadratically with the number of the elements [4].

Equation (3) can be rewritten to account for a possible direct path between the Tx and the Rx, as follows:

$$s_{rx} = \frac{s_{tx}\lambda}{4\pi}\left(\frac{\sqrt{G_d}}{d_d} e^{-jkd_d} + \frac{\lambda\sqrt{G}}{4\pi d_{tx} d_{rx}} \sum_{m=1}^{M}\sum_{n=1}^{N} e^{j\left(\varphi_{m,n} - k\left(d_{tx_{m,n}} + d_{rx_{m,n}}\right)\right)}\right) \quad (8)$$

where d_d is the distance between Tx and Rx and G_d is the overall direct path gain.

Then, the optimal RIS phase can be obtained as:

$$\varphi_{m,n} - k\left(d_{tx_{m,n}} + d_{rx_{m,n}}\right) = -kd_d \quad (9)$$

$$\rightarrow \varphi_{m,n} = k\left(d_{tx_{m,n}} + d_{rx_{m,n}} - d_d\right) \quad (10)$$

Therefore, the received signal is finally given by:

$$s_{rx} = \frac{s_{tx}\lambda}{4\pi}\left(\frac{\sqrt{G_d}}{d_d} + \frac{NM\sqrt{G}\lambda}{4\pi d_{tx} d_{rx}}\right) e^{-jkd_d} \quad (11)$$

III. Phase Quantization Effect

A. On the recived signal level

First, we analyze the scenario without a direct path between Tx and Rx. Using *i*-bit phase quantization leads to a uniformly distributed random phase quantization error $\psi_{m,n} \sim U\left(-\frac{\pi}{2^i}, \frac{\pi}{2^i}\right)$. So, this phase error is added to equation (6):

$$\varphi_{m,n} = k\left(d_{tx_{m,n}} + d_{rx_{m,n}}\right) + \psi_{m,n} \quad (12)$$

Consequently, the received signal is given by:

$$s_{rx_q} = \frac{s_{tx}\sqrt{G}\lambda^2}{(4\pi)^2 d_{tx} d_{rx}} \sum_{m=1}^{M}\sum_{n=1}^{N} e^{j\psi_{m,n}} \quad (13)$$

We are interested in the expected value of this signal. Therefore:

$$E_{\psi_{m,n}}\left(s_{rx_q}\right) = \frac{s_{tx} NM\sqrt{G}\lambda^2}{(4\pi)^2 d_{tx} d_{rx}} sinc\left(\frac{\pi}{2^i}\right) \quad (14)$$

And the normalized signal level (relative to the obtained value without quantization error) is given by:

$$S_{relative} = \frac{E_{\psi_{m,n}}\left(s_{rx_q}\right)}{s_{rx}} = sinc\left(\frac{\pi}{2^i}\right) \quad (15)$$

Equation (15) shows that the relative signal level is independent of the number of RIS elements. This is conditioned by having enough RIS elements so that the phase quantization error has a fine uniform distribution. By simulations, this is found to hold starting from 225 elements. This equation also shows that in the absence of a direct path, the relative signal level is constant and independent of system parameters.

It can easily be deduced that in the case there is also a direct path between Tx and Rx, the received signal in the case of a quantized-phase RIS is given by:

$$s_{rx_q} = \frac{s_{tx}\lambda}{4\pi}\left(\frac{\sqrt{G_d}}{d_d} + \frac{NM\sqrt{G}\lambda}{4\pi d_{tx} d_{rx}} sinc\left(\frac{\pi}{2^i}\right)\right) e^{-jkd_d} \quad (16)$$

Consequently, the normalized signal level is given by:

$$S_{relative} = \frac{\frac{\sqrt{G_d}}{d_d} + \frac{NM\sqrt{G}\lambda}{4\pi d_{tx} d_{rx}} sinc\left(\frac{\pi}{2^i}\right)}{\frac{\sqrt{G_d}}{d_d} + \frac{NM\sqrt{G}\lambda}{4\pi d_{tx} d_{rx}}} \quad (17)$$

As it can be seen, in this case, the relative signal level depends on system parameters (carrier frequency/wavelength, Tx power, Tx and Rx antenna gains, RIS element pattern, Tx-Rx distance, Tx-RIS-Rx).

B. On the channel estimation accuracy

In [13], the authors proposed an optimal method for channel estimation in RIS-aided wireless communications. This method assumes that the RIS is configured using orthogonal configurations during the channel estimation phase by using different rows from a DFT matrix. However, the realization of the DFT matrix requires very fine control of the RIS-phases; for *L*-elements RIS, the phase step of the DFT matrix is given by $\Delta\emptyset = \frac{2\pi}{L}$. Therefore, for a 400-elements RIS, the required RIS phase granularity is around 0.9°. The realization such granularity is almost practically impossible. So we need to quantize these phases in a reasonable range. This quantization breaks the orthogonality of the DFT matrix and degrades the performance of the channel estimation. However, we will show via simulations that starting from 2-bit quantization the channel can still be estimated with very little degradation.

We consider a Single Input Single Output (SISO) communication system assisted by a RIS and Time Division Duplex (TDD) mode. The Rx performs channel estimation based on the known pilot symbols x_l transmitted by Tx and by tuning the RIS phases using different DFT column $\boldsymbol{\gamma}_l$ for each step *l*. If we consider that there is no direct path between Tx and Rx, the received signal model during the training step *l* is then as follows:

$$s_l = \boldsymbol{\theta}_l \boldsymbol{h} + n_l \quad (18)$$

where $\boldsymbol{\theta}_l = x_l \boldsymbol{\gamma}_l^T$, $\boldsymbol{h}$ and $\boldsymbol{\gamma}_l$ are respectively column vectors of size *L* of the cascaded channel gains and the RIS reflection coefficients, n_l is the Additive White Gaussian Noise (AWGN). This equation can be written in the matrix form as:

$$\boldsymbol{s} = \boldsymbol{\Theta h} + \boldsymbol{n} \quad (19)$$

where $\boldsymbol{\Theta} = diag(\boldsymbol{x})\boldsymbol{\Gamma}^T$, $\boldsymbol{s}$ is the received signal vector, $\boldsymbol{x}$ is the known pilot symbols vector, $\boldsymbol{\Gamma}$ is the complete DFT matrix, and $\boldsymbol{n}$ is the noise vector.

The channel can be estimated using a Least Square (LS) estimator, by setting the noise equal to zero in (19), as:

$$\widehat{\boldsymbol{h}}_{LS} = (\boldsymbol{\Theta}^H \boldsymbol{\Theta})^{-1} \boldsymbol{\Theta}^H \boldsymbol{s} \quad (20)$$

The LS-based channel estimation has low computational complexity but a poor performance for low SNRs. So, it can be improved using a Linear Minimum Mean Square Error (LMMSE) estimator, which has better performances but also higher computational complexity, as:

$$\widehat{\boldsymbol{h}}_{LMMSE} = \boldsymbol{R}_{HH}\left(\boldsymbol{R}_{HH} + \frac{\boldsymbol{I}}{SNR}\right)^{-1} \widehat{\boldsymbol{h}}_{LS} \quad (21)$$

where $\boldsymbol{R}_{HH}$ is the channel correlation matrix and **I** is the identity matrix.

Finally, in the case where there is a direct path between Tx and Rx, the received signal model is given by:

$$\boldsymbol{s} = \boldsymbol{\Theta h} + \boldsymbol{x} h_d + \boldsymbol{n} \quad (22)$$

where h_d is the direct path channel gain.

In this case, the channel estimation can be performed in two steps. First, the direct channel is estimated by turning off the RIS, so the received signal is given by:

$$s = x h_d + n \quad (23)$$

Hence, using an LS estimator the direct path is given by:

$$\hat{h}_{d_{LS}} = x^{-1} s \quad (24)$$

In the second step, the RIS is turned on to estimate the entire cascaded channel by subtracting the direct path signal from the received signal as follow:

$$\widehat{\boldsymbol{h}}_{LS} = (\boldsymbol{\Theta}^H \boldsymbol{\Theta})^{-1} \boldsymbol{\Theta}^H \left(\boldsymbol{s} - \boldsymbol{x}\hat{h}_{d_{LS}}\right) \quad (25)$$

IV. Simulation Results

A. Continuous-phase RIS

Let us consider a RIS in the YoZ plane and a Tx and Rx in the XoY plane as shown in Figure 1. This RIS, of a 21×21 elements, is designed for 3.75 GHz 5G's band and with an inter-element distance of half a wavelength. Using spherical coordinate system $(r, \theta, \emptyset)$, the RIS is centered at $(0m, 0°, 0°)$ and Tx is located at $(40m, 90°, -10°)$. Four scenarios are simulated for different Rx locations: $(160m, 90°, -30°)$, $(120m, 90°, 0°)$, $(100m, 90°, 30°)$ and $(140m, 90°, 60°)$. We assume that there is no direct path between Tx and Rx and that Tx, Rx and RIS elements have omnidirectional patterns. Figure 2 shows the required phase calculated for every RIS element for the four different Rx locations. Figure 3 shows the relative received power (normalized to have a maximum value of 0 dB) in the horizontal plane (XoY plane). As it can be seen, in all scenarios (corresponding to the four different Rx locations), the received power is maximized in Rx direction (a beam is successfully formed in Rx direction). Figure 4 illustrates also the obtained pattern in the horizontal plane, calculated by taking the power level on a circle centered at the RIS center and passing by Rx location. The Half Power Beamwidth (HPBW) (i.e., the angle at which the power reduces by 3 dB from its maximum value, on both sides of the maximum

value) in the horizontal plane for the four Rx locations is respectively around 5.6°, 4.8°, 5.6° and 9.8°. This means that, as expected, the best beam formation is achieved in the RIS axis (i.e., for $\emptyset = 0°$). The HPBW in the vertical plane for the four scenarios is 4.8° (the figure is not shown). The Side Lobe Level (SLL) in the horizontal plane for the four scenarios is -13.2 dB. The SLL in the vertical plane for the four scenarios is -13.2 dB (the figure is not shown).

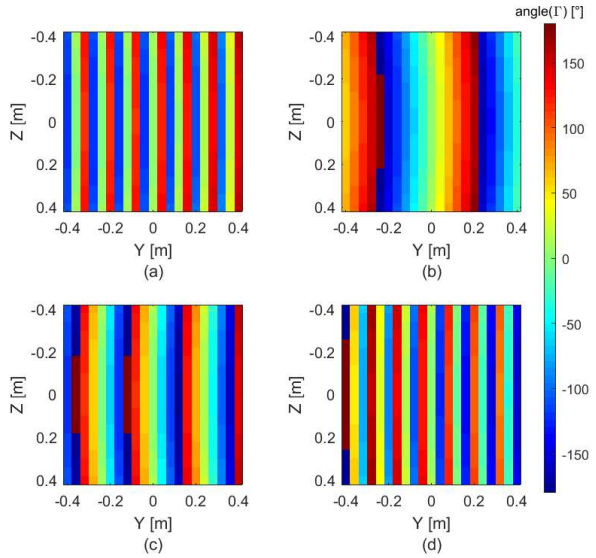

Figure 2. Required RIS phases in the 4 different cases. (a) Case 1, (b) case 2, (c) case 3 and (d) case 4.

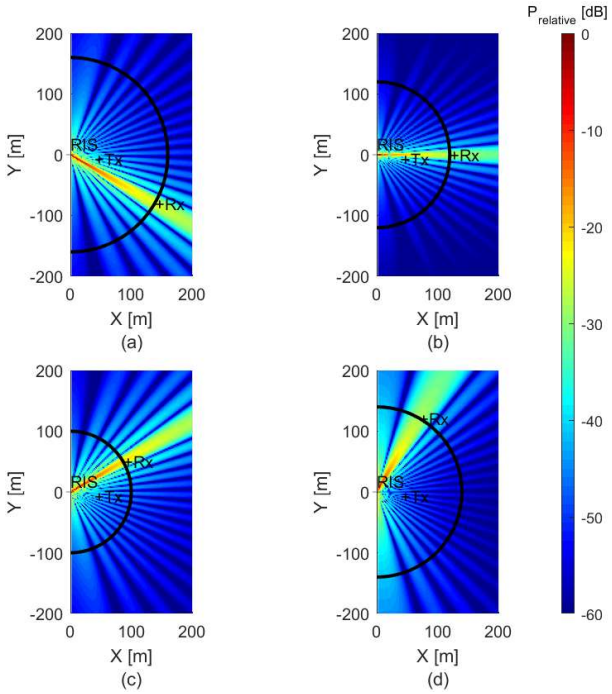

Figure 3. Relative received power in the horizontal plane in the 4 different cases. (a) Case 1, (b) case 2, (c) case 3 and (d) case 4.

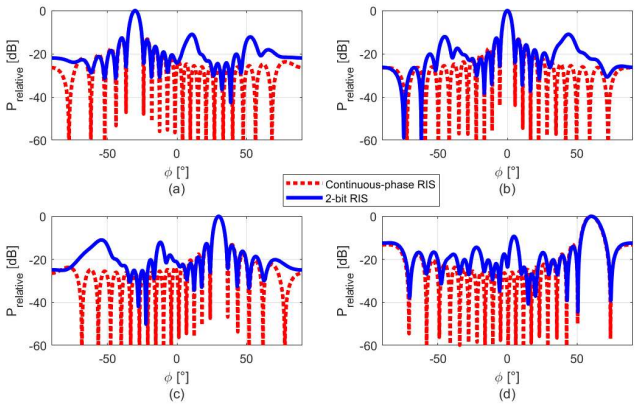

Figure 4. RIS pattern in the horizontal plane in the 4 different cases. (a) Case 1, (b) case 2, (c) case 3 and (d) case 4.

B. Quantized-phase RIS

We repeated the previous simulations taking into account a quantized-phase RIS while varying the number of phase quantization bits from 1 to 10. For example, the RIS phases for 2-bit quantized RIS are recalculated and shown in Figure 5. The relative received power in the horizontal plane in this case is also shown in Figure 6. It can be seen, a beam is still successfully formed in Rx direction despite using a 2-bit quantized RIS. However, higher side lobes appear in some directions. The HPBW in the horizontal plane for the four scenarios is respectively around 5.6°, 4.9°, 5.6° and 9.8°. The HPBW in the vertical plane is around 4.8°. The SLL in the horizontal plane is -11 dB, -11 dB, -11 dB and -9.3 dB. The SLL in the vertical plane is -13.3 dB, -13.2 dB, -13.1 dB and -13.2 dB. These results (HPBW and SLL) are similar to the ones obtained in the continuous-phase RIS case. Figure 7 shows the effect of the number of the bits used for RIS phase quantization on the relative received power in the four cases compared to the analytical results, equation (15). The simulation results are in excellent agreement with the analytical results. This result shows that the use of a 2-bit RIS results in a received power reduction of less than 1 dB. Furthermore, a quasi-optimal performance (less than 0.1 dB power decrement) can be achieved starting from 4-bits (16-setps) quantization.

We re-simulated the same scenarios, this time assuming that there is also a direct path between the transmitter and the receiver. Figure 8 shows the effect of the number of bits used for RIS phase quantization on the relative received power, for the four scenarios, compared to the analytical results. Again, the simulation results are in excellent agreement with the analytical results and very good performances (less than 0.1 dB loss) can be obtained starting from 2-bit quantization. It is worth mentioning that the difference between results of the four scenarios, in presence of a direct path, is due to the dependence of the relative received power on the system parameters, as shown in equation (17).

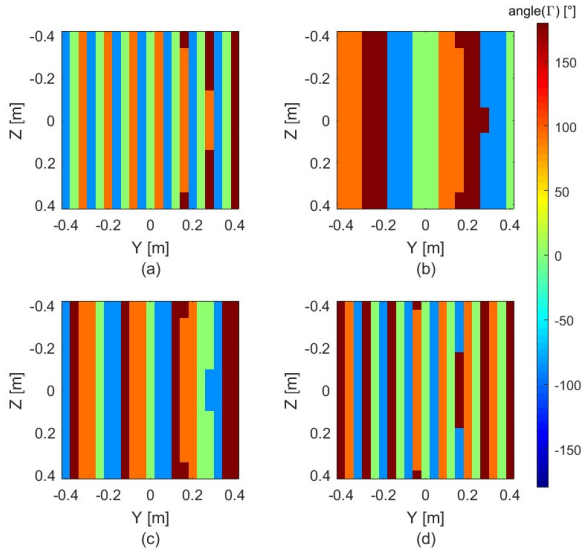

Figure 5. Required 2-bit RIS phases in the 4 different cases. (a) Case 1, (b) case 2, (c) case 3 and (d) case 4.

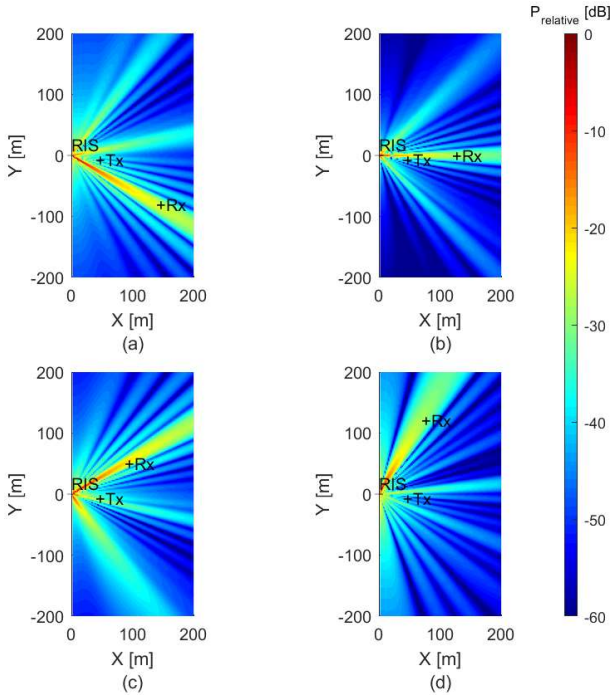

Figure 6. Relative received power in the horizontal plane using a 2-bit RIS in the 4 different cases. (a) Case 1, (b) case 2, (c) case 3 and (d) case 4.

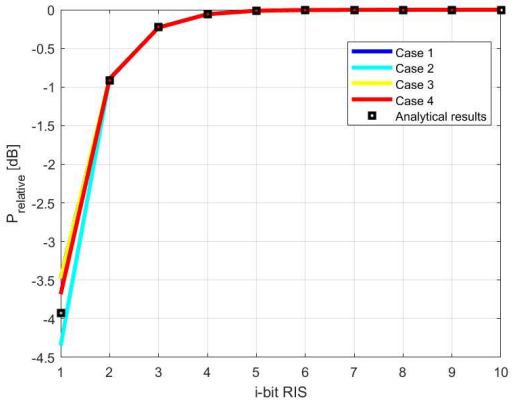

Figure 7. Effect of the quantization step on relative received power.

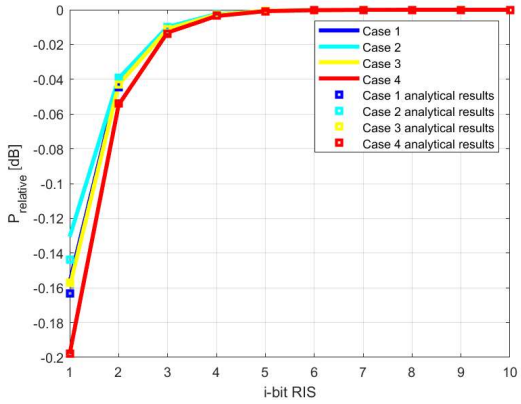

Figure 8. Effect of the quantization step on relative received power when there is a direct path between Tx and Rx.

C. Channel estimation

For channel estimation, we have chosen the fourth scenario mentioned above, which corresponds to Tx and Rx located respectively at (40m,90°,-10°) and (140m,90°,60°) and have used the method detailed in section III-b; assuming an AWGN channel and considering two scenarios with and without a direct path between Tx and Rx. We first simulated the case of 1-bit quantization, revealing that the channel cannot be estimated in this case because the configuration matrix (the deformed DFT matrix) is close to singular or badly scaled. Then, we simulated the case of 2-bit quantization. Three estimators were studied: LS and two LMMSEs, one using perfect Channel State Information (CSI) and the other using the estimated LS channel to calculate the channel correlation matrix. The obtained results in terms of Normalized Mean Square Error (NMSE) are shown in Figure 9. It can be seen that in this case the channel can be estimated with very little degradation compared to the continuous-phase RIS. Indeed, in absence of a direct path between Tx and Rx, to obtain the same NMSE in the two cases (quantized-phase RIS and continuous phase RIS), the SNR of quantized-phase RIS has to be increased by around 1.5 dB in the cases of LS and LMMSE with using the estimated LS channel for calculating the channel correlation matrix and less than 0.25 dB in the case of LMMSE using perfect CSI for calculating the channel correlation matrix. It should be noted that the SNR shown in Figure 9 for the case of existing direct path between Tx and Rx is the SNR of the indirect signal only (after removing the direct signal from the total received signal). Indeed, the SNR of the total received signal is 23.24 dB higher.

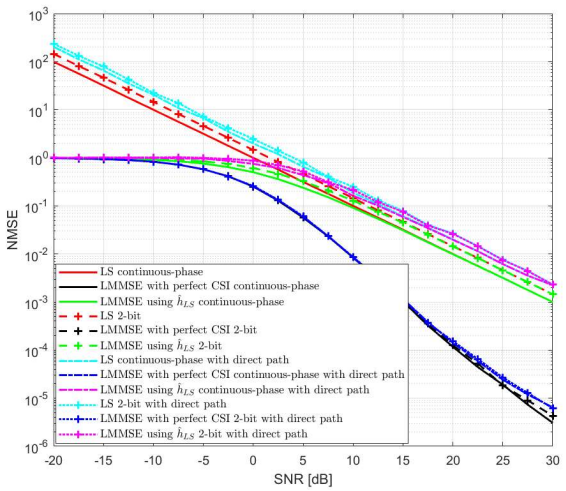

Figure 9. Effect of RIS phase quantization on the channel estimation accuracy.

V. CONCLUSION

In this paper, the effect of the RIS phase quantization on wireless system performances has been investigated both analytically and by simulations. It has been shown that using a phase-quantized RIS (starting from 2 bits) can still yield very good performances in terms of received power level, HPBW, and SLL. For example, in the case there is no direct path between Tx and Rx, using a 2-bit RIS results in less than 1 dB loss in the received power level and little degradation in the SLL compared to a continuous-phase RIS. It also results in a very small degradation in the channel estimation accuracy.

ACKNOWLEDGMENT

This work has been partly funded by the European Commission through the H2020 project Hexa-X (Grant Agreement no. 101015956).

REFERENCES

[1] V. Tapio, I. Hemadeh, A. Mourad, A. Shojaeifard, and M. Juntti, "Survey on Reconfigurable Intelligent Surfaces below 10 GHz", EURASIP Journal on Wireless Communications and Networking, 2021.

[2] E. Basar, "Present and Future of Reconfigurable Intelligent Surface-Empowered Communications", IEEE Future Networks 1st Massive MIMO Workshop, November 2021.

[3] M. M. Amri, N. M. Tran, and K. W. Choi, "Reconfigurable Intelligent Surface-Aided Wireless Communications: Adaptive Beamforming and Experimental Validations", IEEE Access, vol. 9, pp. 147442-147457, 2021.

[4] E. Björnson, H. Wymeersch, B. Matthiesen, P. Popovski, L. Sanguinetti, and E. de Carvalho, "Reconfigurable Intelligent Surfaces: A Signal Processing Perspective with Wireless Applications", in IEEE Signal Processing Magazine, vol. 39, no. 2, pp. 135-158, March 2022.

[5] X. Pei, H. Yin, L. Tan, L. Cao, Z. Li, K. Wang, K. Zhang, and E. Björnson, "RIS-Aided Wireless Communications: Prototyping, Adaptive Beamforming, and Indoor/Outdoor Field Trials", in IEEE Transactions on Communications, vol. 69, no. 12, pp. 8627-8640, December 2021.

[6] C. Pan, H. Ren, K. Wang, J. F. Kolb, M. Elkashlan, M. Chen, M. Di Renzo, Y. Hao, J. Wang, A. L. Swindlehurst, X. You, and L. Hanzo, "Reconfigurable Intelligent Surfaces for 6G Systems: Principles, Applications, and Research Directions", in IEEE Communications Magazine, vol. 59, no. 6, pp. 14-20, June 2021,

[7] R. Liu, G. C. Alexandropoulos, Q. Wu, M. Jian, and Y. Liu, "How Can Reconfigurable Intelligent Surfaces Drive 5G-Advanced Wireless Networks: A Standardization Perspective", IEEE/CIC International Conference on Communications in China, Sanshui, Foshan, China, 2022, pp. 221-226, 2022.

[8] R. Liu, Q. Wu, M. Di Renzo, and Y. Yuan, "A Path to Smart Radio Environments: An Industrial Viewpoint on Reconfigurable Intelligent Surfaces", IEEE Wireless Communications, vol. 29, no. 1, pp. 202-208, February 2022.

[9] R. Liu, J. Dou, P. Li, J. Wu, and Y. Cui, "Simulation and Field Trial Results of Reconfigurable Intelligent Surfaces in 5G Networks", in IEEE Access, vol. 10, pp. 122786-122795, 2022.

[10] Q. Wu, and R. Zhang, "Beamforming Optimization for Wireless Network Aided by Intelligent Reflecting Surface With Discrete Phase Shifts", IEEE Transactions on Communications, vol. 68, no. 3, pp. 1838-1851, March 2020.

[11] J. Kim, H. Yu, X. Kang, and J. Joung, "Discrete Phase Shifts of Intelligent Reflecting Surface Systems Considering Network Overhead", Entropy 2022.

[12] C. A. Balanis, "Antenna Theory Analysis and Design", 3rd edition, Wiley-Interscience, 2005.

[13] T. L. Jensen, and E. De Carvalho, "An Optimal Channel Estimation Scheme for Intelligent Reflecting Surfaces Based on a Minimum Variance Unbiased Estimator", IEEE International Conference on Acoustics, Speech and Signal Processing (ICASSP), pp. 5000-5004, Barcelona, Spain, 2020.